ORIGINAL PAPER

Ancient Roman wall paintings mapped nondestructively by portable NMR

Agnes Haber · Bernhard Blümich · Daria Souvorova · Eleonora Del Federico

Abstract The stratigraphies of decorated walls in ancient Herculaneum, Italy, were analyzed by single-sided ^{1}H NMR. A large version of the NMR-MOUSE® with a maximum penetration depth of 25 mm was used to map proton density profiles at different positions of the Mosaic of Neptune and Amphitrite showing considerable differences between different tesserae and the mortar bed at different times of the year. In the House of the Black Room, different mortar layers were observed on painted walls as well as different proton content in different areas due to different moisture levels and different conservation treatments. The proton density profiles of the differently treated areas indicated that one method leads to higher moisture content than the other. Untreated wall paintings from different times were profiled in a recently excavated room at the Villa of the Papyri showing two different types of mortar layer structures which identify two different techniques of preparing the walls for painting. Reflectance Fourier mid-infrared spectroscopy and in situ X-ray fluorescence measurements complemented the NMR measurements and provided additional insight into the identification of organic coatings as well as the nature of the

pigments used, respectively. The information acquired nondestructively by NMR is valued for elaborating conservation strategies and for identifying different schools of craftsmen who prepared the mortar supports of the wall paintings.

Introduction

Nuclear magnetic resonance (NMR) is a physical resonance phenomenon of magnetic atomic nuclei that precess in a magnetic field [1]. It is made use of for the analysis of matter in a variety of ways with various applications in medicine, chemistry, materials science, geophysics, and chemical engineering [2, 3]. In conventional NMR, massive, superconducting magnets with field strengths of up to 22 T are used to obtain high sensitivity. Since the object of interest needs to be located inside, these magnets are not suitable for nondestructive analysis of large objects. Also, such magnets cannot be transported easily, as they are heavy and must be cooled with liquid nitrogen and liquid helium. This is why mobile permanent magnets were introduced to materials testing where the object of interest is positioned in the stray field outside the magnet. The first small device of this kind was the NMR Mobile Universal Surface Explorer or NMR-MOUSE® [4]. The sensor employs a U-shaped permanent magnet with a radio-frequency (rf) coil in the gap between the two magnetic poles (Electronic Supplementary Material, Fig. S1). This arrangement of magnet and coil creates a sensitive volume outside of the sensor, from which the signal is received. For

A. Haber · B. Blümich (✉)
Institute for Technical and Macromolecular Chemistry,
RWTH Aachen University,
Worringer Weg 1,
52056 Aachen, Germany
e-mail: bluemich@mc.rwth-aachen.de

D. Souvorova · E. Del Federico
Pratt Institute, Department of Mathematics and Science,
200 Willoughby Ave,
Brooklyn, NY 11205, USA

the Profile NMR-MOUSE, this sensitive volume is a flat slice of about 1 cm diameter parallel to the surface of the sensor [5].

In order to acquire depth profiles, the distance between sensor and object is changed in appropriate steps and the sensitive volume is shifted through the object along the depth direction. This method can be applied to all objects which contain hydrogen nuclei and are neither electrically conductive nor magnetic. Depending on the penetration depth, different sensors are available [6]. The greater the penetration depth, the larger is the sensor. Standard depths are 3, 10, and 25 mm. Since the magnetic field decreases with increasing distance from the sensor, the field strength of sensors with larger depth access is smaller than that of sensors for smaller depth access. At the same time, the intensity of the received signals decreases with increasing depth. This loss is balanced for sensors with high depth access by an increase of the sensitive volume in width and thickness. This, in turn, affects the depth resolution, so that for layers of paint and paper the 3-mm sensor is used, for wood and bones, the 10-mm sensor, and for moisture in building materials, the 25-mm sensor.

For the measurements, the NMR-MOUSE is mounted on a precision lift, whose position is controlled by a computer. Then the assembly is positioned close to the object in such a way that the sensitive slice is parallel to the object. The measurement starts with the smallest distance between sensor and object at the largest measurement depth, and then the sensor is retracted step by step. At each depth, an NMR signal is received, from which a number is computed which determines the amplitude in a depth profile (Electronic Supplementary Material, Fig. S2). Sensors with small depth access can provide spatial resolution better than 10 μm [5]. The Profile NMR-MOUSE has been employed for nondestructive testing of different types of objects of cultural heritage [7] including investigations of the layer structure of paintings [8, 9], the degradation of paper [10–13], measurements of bones and mummies [14], porous materials [15–18], and the moisture distributions of wood [19] and wall paintings [8, 9, 20].

Herculaneum is an ancient city in the bay of Naples which became Roman municipium under Titus Didius in 89 BC. In 62 AD, an earthquake destroyed parts of the city, and in 79 AD, it was completely buried under volcanic material by the eruption of the volcano Vesuvius. The best known residence is the Villa of the Papyri which owes its name to a library of 1,800 papyrus scrolls found in the Villa during the eighteenth century. Excavations of Herculaneum started in 1737 and while they have lead to a wealth of information about the Roman life in general, they have also brought deterioration and a generalized decay of the site, its precious wall paintings, and mosaics. In 2001, the Herculaneum Conservation Project was launched in order to address and halt the serious decay conditions found at the site [21].

Moisture is a key concern in Herculaneum especially in the conservation of the wall paintings and mosaics. Moisture triggers the leaching of salt ions from the ground, building materials, as well as from depositions of a polluted atmosphere or from biological activity which are then transported through the walls by capillary forces. Transported salts can accumulate in areas of water evaporation, and once saturation is reached, they precipitate. Salts generally become concentrated on the surface of paintings as efflorescences or below the surface as sub-efflorescences. The highest damage is caused when salts precipitate below the paint layer as it causes the painting to flake and disintegrate. Gypsum ($CaSO_4 \cdot 2H_2O$) is one of the most damaging salts present in deteriorated wall paintings, and most wall painting restoration procedures have been developed to remove this salt followed by the reconsolidation of the wall [22, 23]. It is now known that the organic consolidants used in early conservation treatments cause more damage in the long term because they occlude the natural porosity of a wall painting and interfere with salt transport, causing salt precipitation where it otherwise would not occur. Therefore the use of inorganic substances, such as barium hydroxide, or ammonium oxalate for the consolidation of mural paintings is favored over treatments with primarily organic substances [23]. Moreover, the identification of past restoration efforts is equally as important as the assessment of the conservation state, and the effectiveness of new conservation treatments.

This work reports experimental results about the stratigraphy of decorated walls in ancient Herculaneum. Depth profiles were recorded for the Mosaic of Neptune and Amphitrite, and for wall paintings in the House with the Black Room and the Villa of the Papyri. These measurements form an exploratory study to identify the type of information available from unilateral NMR with the NMR-MOUSE and their significance to the conservation and restoration of mosaics and wall paintings.

Experimental

A typical measurement with the NMR-MOUSE applies a string of rf impulses. The first impulse invokes an impulse response, which decays rapidly owing to the inhomogeneity of the stray field of the NMR magnet. Echoes of the original impulse response are recalled many times with the subsequent rf impulses. This way of measuring is referred to as the CPMG method according to its discoverers Carr, Purcell, Meiboom, and Gill (Electronic Supplementary Material, Fig. S2) [24, 25]. The envelope of the CPMG

echo train is recorded [2]. It decays with time. Its initial amplitude provides the proton density, which is proportional to the content of water and organic material in the walls. The decay-time constant T_2 varies with the mobility of the protons. The protons in dry binders of paint layers have short T_2, whereas those in liquid bulk water have long T_2. Consequently, the NMR signal from paint and bound water in mortar decays quickly, often in less than 1 ms; whereas, moist walls may provide NMR signals lasting tens of milliseconds.

The experimental CPMG signal $s(t)$ can be processed in different ways. A good approximation of the signal is a sum of many exponential functions with relaxation times $T_{2\text{eff},i}$

$$\frac{s(t)}{s(0)} = \sum_i x_i \exp\left\{\frac{-t}{T_{2\text{eff},i}}\right\}, \tag{1}$$

where x_i is the relative spin density or mole fraction of components with the relaxation times $T_{2\text{eff},i}$ in the sensitive volume. Often used is also the contrast parameter w. It is defined by the ratio of partial integrals over $s(t)$,

$$w = \int_{t_1}^{\infty} s(t)\,\mathrm{d}t \Big/ \int_{0}^{t_1} s(t)\,\mathrm{d}t. \tag{2}$$

The NMR measurements were executed with a Profile NMR-MOUSE® giving 21 mm depth access at a proton resonance frequency of 13.86 MHz. The measurements of the Mosaic of Neptune and Amphitrite and of the wall paintings at the Villa of the Papyri were recorded with a 5-mm spacer between the sensor and the rf coil to reduce the depth access to 16 mm for the benefit of improved sensitivity. For the measurements in the Black Room, a 15-mm spacer was introduced to gain even higher sensitivity at the expense of the depth access being reduced to 6 mm. The sensor was mounted on a computer-driven positioning device. The NMR sensor and the positioning device were manufactured by ACT GmbH, Aachen, Germany. The spectrometer was a Kea spectrometer manufactured by Magritek Ltd, New Zealand, connected to a Dressler 1 kW rf amplifier. The measurement parameters of all experiments are summarized in Table 1.

The NMR measurements were complemented with reflectance Fourier transform mid-infrared spectroscopy (FTIR) and X-ray fluorescence (XRF) measurements. These techniques were applied in situ with portable instrumentation. The FTIR spectra were recorded using a Bruker Optics ALPHA FTIR spectrometer equipped with an external reflection probe. Each spectrum was accumulated from 1,800 scans with a resolution of 4 cm^{-1} in a range of 400 to 4,000 cm^{-1}. The spectrometer was fitted with a permanently aligned interferometer based on a Bruker Optics patented RockSolid™ design and a DLATGS detector operating at room temperature. Recently, reflectance FTIR analysis has been shown to be very valuable for the in situ, nondestructive analysis of the organic material present on wall paintings [26–28]. Although reflectance FTIR spectra are much more difficult to interpret than the widely used transmission spectroscopy, the possibility to measure them nondestructively and in situ makes this approach worthwhile for the present studies. The X-ray fluorescence measurements were taken in situ using a Bruker AXS Tracer III/IV® portable unit either under vacuum conditions with a voltage of 40 kV and a current of 1.2 μA or with Al-Ti-Cu-filtered Rhodium radiation using a voltage of 14 kV and a current of 1.5 μA. The first setting allowed the detection of elements of atomic number 13 (Al) or higher, whereas the second setting is most efficient in identifying elements above atomic number 20 (Ca).

Mosaic of Neptune and Amphitrite

The mosaic at the house of Neptune and Amphitrite is one of the most famous Roman mosaics, still preserved in its original setting, on the south wall of a triclinium (dining room) of a middle-class household. The room is decorated with wall paintings with garden scenes, a nympheum, giving the illusion of the outdoors. The house lacks a garden, which was a "must" for the Roman elites and therefore the presence of such a richly decorated room suggests that the owner of the house went to high expense to have this room decorated like the elite specially by

Table 1 Acquisition parameters for depth profiles for the measured points

Parameters	Mosaic of Neptune and Amphitrite	House of the Black Room	Villa of the Papyri
Maximum depth [mm]	16	6	16
Pulse width [μs]	21	6.5	19
Echo time [μs]	140	145	140
Number of echoes	16	16	256/64
Number of scans	512	256	32/64
Time/profile [min]	80	60	90

commissioning a mosaic made of expensive polychrome tesserae.

The mosaic was examined twice in 2009. Two regions can be identified in the profiles, one from 0 to 6 or 7 mm depth and one from higher depths. They are assigned to the tesserae with some mortar between them and to the mortar embedding the tesserae, respectively. Points 1 and 2 were measured in March, and all other points including point 1 were measured in October (Fig. 1a). Thus, point 1 was measured twice to investigate reproducibility and the influence of seasonal moisture variation. The measurement points were chosen depending on the nature of the tesserae and their height from the bottom of the mosaic, as both facts may have an impact on the moisture content.

The depth profiles shown in Fig. 1b compare extreme cases in terms of the absolute sums of the first few echoes. The two profiles obtained for point 1 six months apart, overlap almost identically in the region of the tesserae from 0 to 7 mm, while they differ at higher depths. There, the amplitude of the profile measured in fall is lower than that of the profile measured in spring. This can be explained with the wall being dryer in fall than in spring. This interpretation is supported by the fact that points 1 and 2 show identical profiles for the mortar bed. In fact, both points are at the same height from the ground (Fig. 1a). The profiles from all points other than point 1 overlap well in

the region of the tesserae (Fig. 1c). Significant differences are detected only at higher depths characteristic of the mortar bed. Point 6 is the highest one measured in the mosaic and shows the lowest signal in the mortar region. Point 7, on the other hand, is the lowest and shows the highest mortar signal. Points 3 and 4 are positioned at the same height and overlap in the mortar region. In summary, the higher the measurement position, the lower is the profile amplitude in the region of the mortar. This is a strong indication that the source of moisture is located on the ground.

The T_2 parameter profiles (Fig. 1d) look very different from the amplitude profiles. They peak at the interface between the tesserae and the mortar bed with rather broad maxima. While the amplitude in the regions of the tesserae at point 1 is very intense, the corresponding T_2 values are very low. Together with the perfect overlap of the profile region measured 6 month earlier (Fig. 1b), this is a strong indication that the ^{1}H signal does not derive from water but from an organic coating at the surface, possibly an undocumented early consolidation treatment.

Noteworthy is also the extreme behavior of the amplitude and T_2 profiles at point 7. The signal amplitude increases strongly with depth (Fig. 1b), while the T_2 profile exhibits a narrow peak at the interface between tesserae and mortar bed. This indicates high moisture deeper down
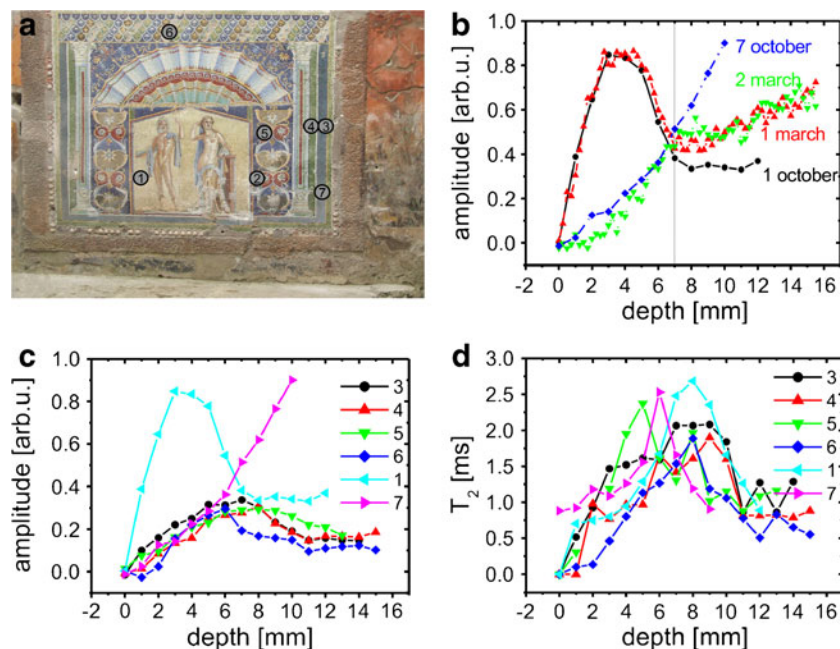

Fig. 1 Mosaic of Neptune and Amphitrite. a) The mosaic with the position of which the NMR depth profiles were acquired. *Point 2* was measured just in March but *point 1* in March and October. b) Depth profiles for *point 1* (*black* and *red*) recorded 6 months apart. The first parts are overlapping identically while the profiles differ inside the mortar bed. The mortar signal from *point 2* (*green*) overlaps perfectly with the mortar signal from *point 1*, both measured in March, evidencing the same moisture conditions for this area of the mortar bed. The depth profile for *point 7* (*blue*) reports a high moisture content of the mortar bed at the lowest point measured. c) Depth profiles for all in March measured points. The moisture content in the mortar is lower at higher distance from the floor. d) T_2 profiles for all measured points

inside the wall and possibly a beginning detachment of the stones from the mortar bed. The tesserae of the mosaic were also investigated at 50 different positions by XRF. These data will be published elsewhere [29, 33].

The Black Room

Across the street from the House of Neptune and Amphitrite is the back entrance to the House of the Black Room, one of the most luxurious ones in Herculaneum with its main entrance overlooking the city's main street, the Decumanus Maximus. The house owes its name to a large room that is decorated with pillars and chandeliers painted with a black background in the third Pompeian style. The room was excavated between 1933 and 1961. Although not documented, it is believed that all wall paintings excavated during that time period were treated with a mixture of bees wax and paraffin as a preventive conservation measure to avoid further damage. Over time, however, changes in relative humidity, the use of modern cement for restoration of the walls, and air pollution have caused damaging salts to leach from the walls and precipitate as efflorescence on the surface or just below the paint layer. This efflorescence has caused significant damage which includes delamination and pulverization of the paintings. The presence of earlier conservation treatments including an organic coating have contributed to this decay. The northwestern wall (wall B) of the main room in the House of the Black Room, behind which a modern Portland cement wall was build, displays the most salt damage with its paint layer delaminated in many areas. Salt efflorescence on this wall concentrates around the area behind which the new wall was built. Recent conservation efforts involved the removal of consolidants from early restorations and application of test treatments in small areas of the cleaned walls.

The three painted walls labeled A, B, and C (Fig. 2a,b) of the room were analyzed in terms of depth profiles at selected positions identified by Prof. Mauro Matteini on account of their different conservation treatments. On walls A and B (Fig. 2a), the measurements were made at points where the organic fixative treatment was still present and at points where it had been removed. On wall C (Fig. 2b) ammonium oxalate and barium hydroxide treatments were tested. To maximize the sensitivity for the measurements at natural proton content, the depth profiles were taken with

Fig. 2 NMR measurements in the Black Room. a) The measurement points were on walls A and B. b) Wall C, where sections have been treated with barium hydroxide and ammonium oxalate. The experimental setup can be recognized. c) Depth profiles for all measured points. Depending on the wall and the conservation technique differences in moisture content are found. d) T_2 profiles for all measured points. All points show mostly the same T_2 value. e) Depth profiles for wall A showing the proton content with and without fixative on the wall painting. f) Depth profiles for wall C showing the difference in proton content for the treatments with barium hydroxide and ammonium oxalate and their comparison with the proton content for an untreated region from the same wall
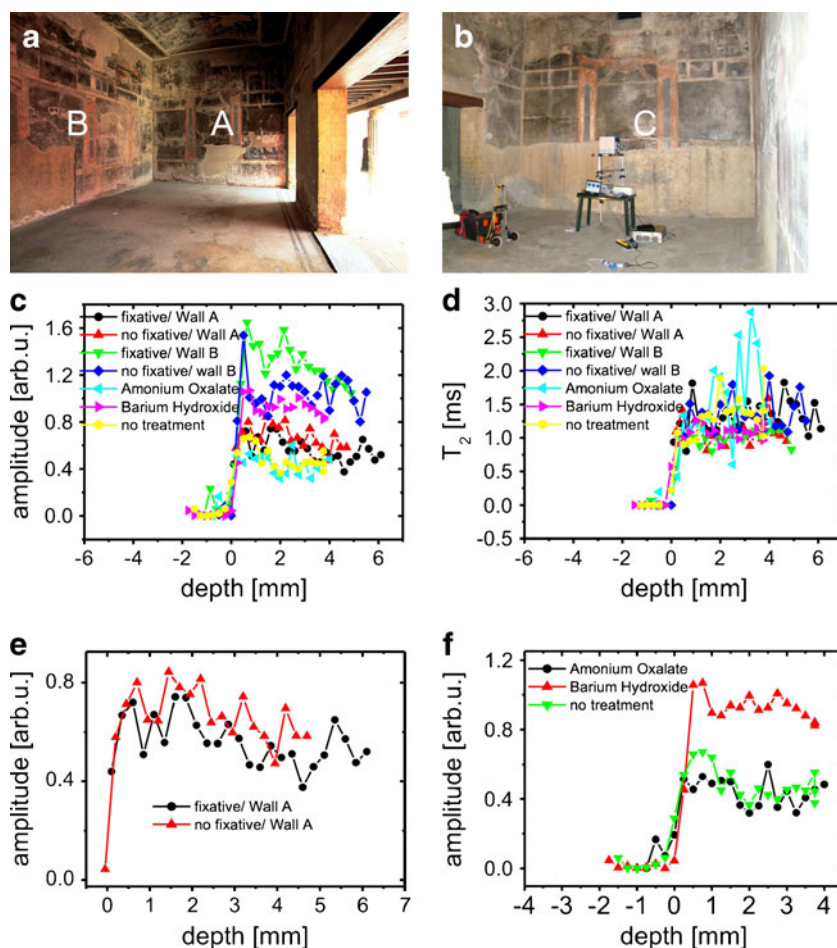
all spacers placed in the magnet. This resulted in a maximum accessible depth of 6 mm.

The proton density profiles (Fig. 2c) differ in the absolute amplitudes but are similar in shape in that they show the highest signal at the surface, a peak at about 2 mm depth with the signal amplitude decreasing with increasing depth. The T_2 profiles (Fig. 2d) show little variation between different positions which is mainly attributed to the low signal-to-noise ratio of the measurement. The profiles acquired on wall A (Fig. 2e) for both the untreated area which is coated with organic consolidants and an area which was treated to remove the organic coating, do not differ much in signal amplitude.

These observations are in good agreement with the reflectance FTIR spectra obtained for both points. FTIR measurements indicate that after treatment (removing the

fixative), there is still significant organic material left on the cleaned surface of wall A. This is indicated by the presence of the C–H bending bands between 3,000–2,800 cm^{-1}, as well as bands in the C=O stretching region at about 1,750 cm^{-1} (Fig. 3a). Together, those signals indicate the presence of either a lipidic or a synthetic coating such as an acrylic resin or the presence of both (Fig. 3b). However the low intensity of the bands in the region of 3,000–2,800 cm^{-1} together with the presence of a band at about 1,160 cm^{-1} for the untreated area of wall A may be an indication that the coating included an acrylic consolidant [26–28]. Furthermore, the bands at 1,750 and 1,160 cm^{-1} decrease in intensity after the application of the cleaning treatment on wall A and an organic coating of a different nature, possibly protein-based remains. This can be inferred from Fig. 3c which overlays this spectrum with the spectra
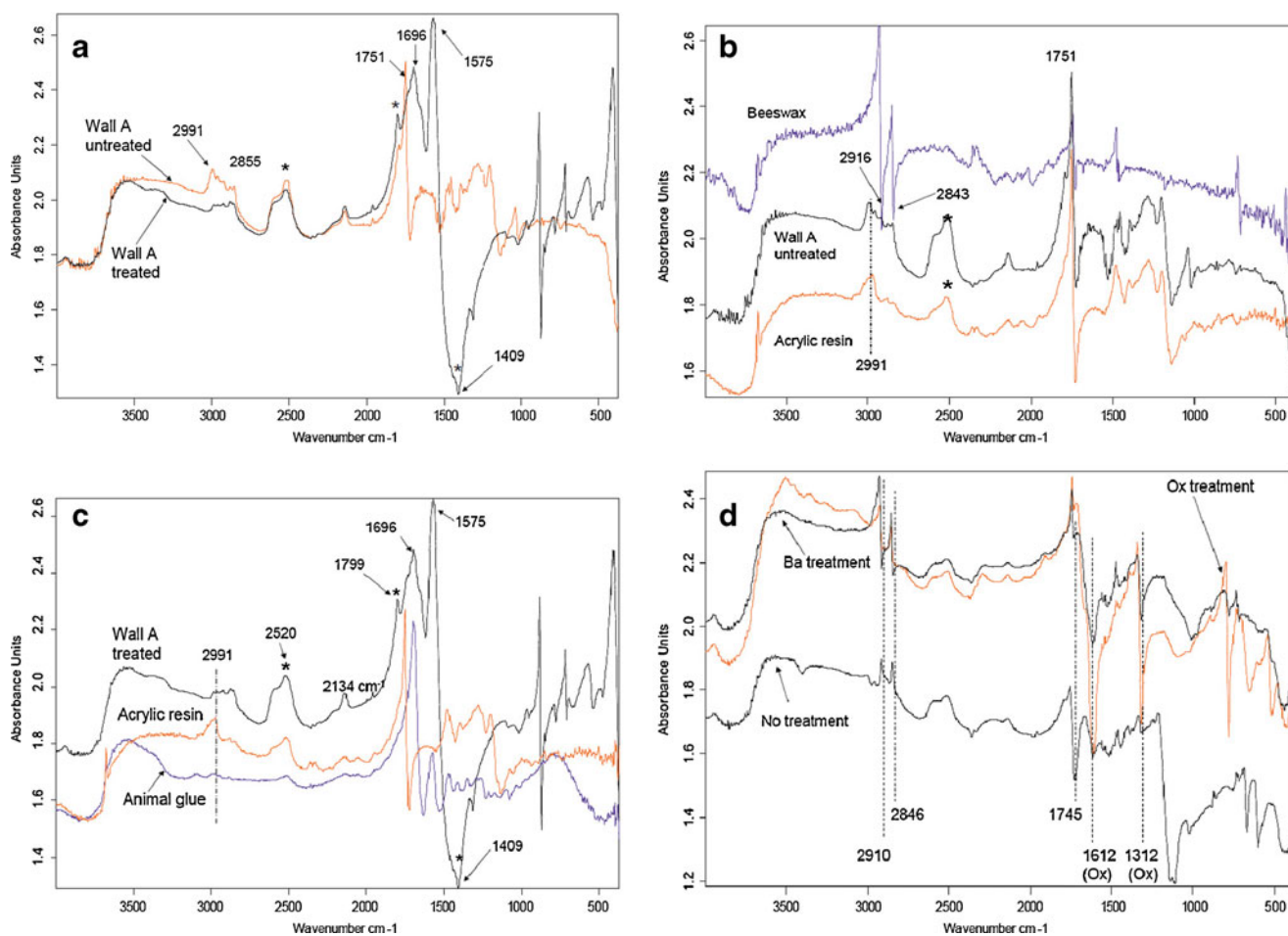

Fig. 3 Reflectance FTIR measurements in the Black Room. a) Comparison of the FTIR spectra of a cleaned area of wall A (red) with the spectra of an untreated area of the same wall (black). b) Comparison of the spectra of the untreated wall A and mock samples prepared with beeswax or acrylic resin, suggesting that wall A is covered by an acrylic resin. c) Comparison of the FTIR reflectance spectra of a cleaned area of wall A with those from mock samples prepared with a coating of acrylic resin or animal glue (a protein). It is

suggested that most of the acrylic resin disappears upon cleaning; however, a possible coating of a protein nature remains due to the presence of peaks at 1,696 and 1,575 cm^{-1}. d) FTIR spectra of the different areas of wall C with and without treatment showing the presence of organic material after treatment (peaks at 2,910, 2,846, and 1,745 cm^{-1}) characteristic of beeswax, and the expected presence of oxalates (at 1,612 and 1,312 cm^{-1}) in the treated area

of mock wall paintings prepared in the laboratory and coated with either animal glue or acrylic resin. The figure clearly indicates the overlap of the animal glue bands with peaks at 1,696 and 1,575 cm^{-1}, which are absent in the acrylic resin spectrum. These bands can be assigned to the characteristic amide I and amide II bands present in the FTIR spectrum of all proteins and absent in acrylic resins. The amide I band is due to the C=O stretching vibrations while the amide II is due primarily to N–H bending vibrations [30]. The presence of calcium carbonate from a fresco matrix can be inferred by the presence of bands at 2,520, 1,795, and 1,409 cm^{-1}, which are more intense upon treatment. The signal at 2,134 cm^{-1} indicates the possible presence of sulfates, which were not visible before the cleaning treatment.

The NMR profiles from wall B show a proton density significantly higher than that in all other profiles from walls A or C. This observation is consistent with the existence of visible salt layers due to the moisture exchange being hindered by the modern concrete wall. For this wall the amplitudes of the profiles measured at locations without organic consolidant treatment and with the consolidant removed are quite different with the exception of the first two profile points at the very surface. There the amplitude is high and the same for both profiles suggesting incomplete removal of the consolidant treatment. The profiles of wall C (Fig. 2f) from a point cleaned to remove the older organic consolidant (no treatment) and from the points with conservation treatments (ammonium oxalate, barium hydroxide) are all very different albeit physically closely spaced. The point where the cleaning was performed shows a profile similar to that at the point treated with ammonium oxalate. However, in the first millimeter, the higher signal is given by the untreated area probably due to incomplete removal of the older treatment. At larger depth, the amplitude of the area treated with the barium hydroxide displays the highest intensity and therefore this is the area with the highest moisture content. Although the higher moisture content in the barium hydroxide treated area may suggest, that the treatment with barium hydroxide is inferior to the treatment with ammonium oxalate, it is not the moisture content but the moisture volume flow rate which should be assessed to rank the effectiveness of the treatments. Such investigations are currently being undertaken by measuring moisture self-diffusion with the NMR-MOUSE. These observations are consistent with laboratory studies of moisture in mock-up mortar beds.

Reflectance FTIR spectra of the uncleaned surface of wall C (Fig. 3d, no treatment) suggest the presence of an acrylic consolidant based on the presence of the characteristic peak at 1,160 cm^{-1} with C–H bending bands between 2,800 and 2,990 cm^{-1}, and the C=O stretching band at about 1,750 cm^{-1}. Furthermore the characteristic peak at

1,160 cm^{-1} disappears on the cleaned surfaces, suggesting the complete removal of the acrylic consolidant but the presence of an earlier organic layer beneath the acrylic treatment, which appears lipidic in nature due to the C=O peaks at 1,740 cm^{-1} and the sharp, second-derivative shape peaks between 2,900–2,800 cm^{-1} [26–28]. This compound probably gives rise to the peaks between 0 and 1 mm in the profiles of Fig. 2f. Furthermore, as expected, upon treatment with ammonium oxalate, one can find the typical peaks for calcium oxalate at ~1,315 cm^{-1} attributed to C–O stretching, and at 1,615 cm^{-1} attributed to C=O stretching.

The Villa of the Papyri

The Villa of the Papyri was first explored from 1750 to 1765 through a network of tunnels burrowed into the volcanic rock by Karl Jacob Weber, a Swiss architect and engineer, under the patronage of Charles III of Spain. From his detailed drawings an accurate map of the villa could be established. Today a large part of the villa remains underground. In 1826, a library of about 1,800 papyrus scrolls was discovered which gave the villa its name. It is believed, that the house belonged to a wealthy and learned Roman noble man, probably Lucius Calpurnius Piso Caesoninus, father in law of Julius Caesar and consul in 58 BC. Recent excavations have unearthed a small room with bright colored wall paintings in a superb state of conservation. This room is therefore of outmost interest to conservators, conservation scientists, archeologists, and historians as its surfaces remain as they were left in 79 AD. It is in this room and on the above terrace where our NMR measurements were taken.

As a benefit to our NMR measurements this room is kept moist at 96% humidity to direct the moisture migration into the walls and keep salts from crystallizing. Two of its walls were examined (Fig. 4a). In all, four positions were studied in detail, three inside the room and one on the outside wall (Fig. 4b) facing the terrace above that room. Interestingly, two types of stratigraphy can be identified, each being represented by two different profiles (Fig. 4c, d). One type was measured at points A and B in a wall dating from the time before the earthquake of 62 AD (Fig. 4a) and the other at a wall rebuilt after the earthquake and the outside terrace wall (Fig. 4b). The amplitude profiles show humps and valleys at similar positions of matching pairs, which reveal the layer structure of the mortar bed. The fabrication of these layers has been described by Vitruvius [31] and more recently in many scientific studies of wall fragments found in different locations [32, 34]. The profiles of the older wall are thicker and more intricate than the ones from the newer wall and the terrace wall. This may be because the more recent method of preparing the mortar for the wall painting
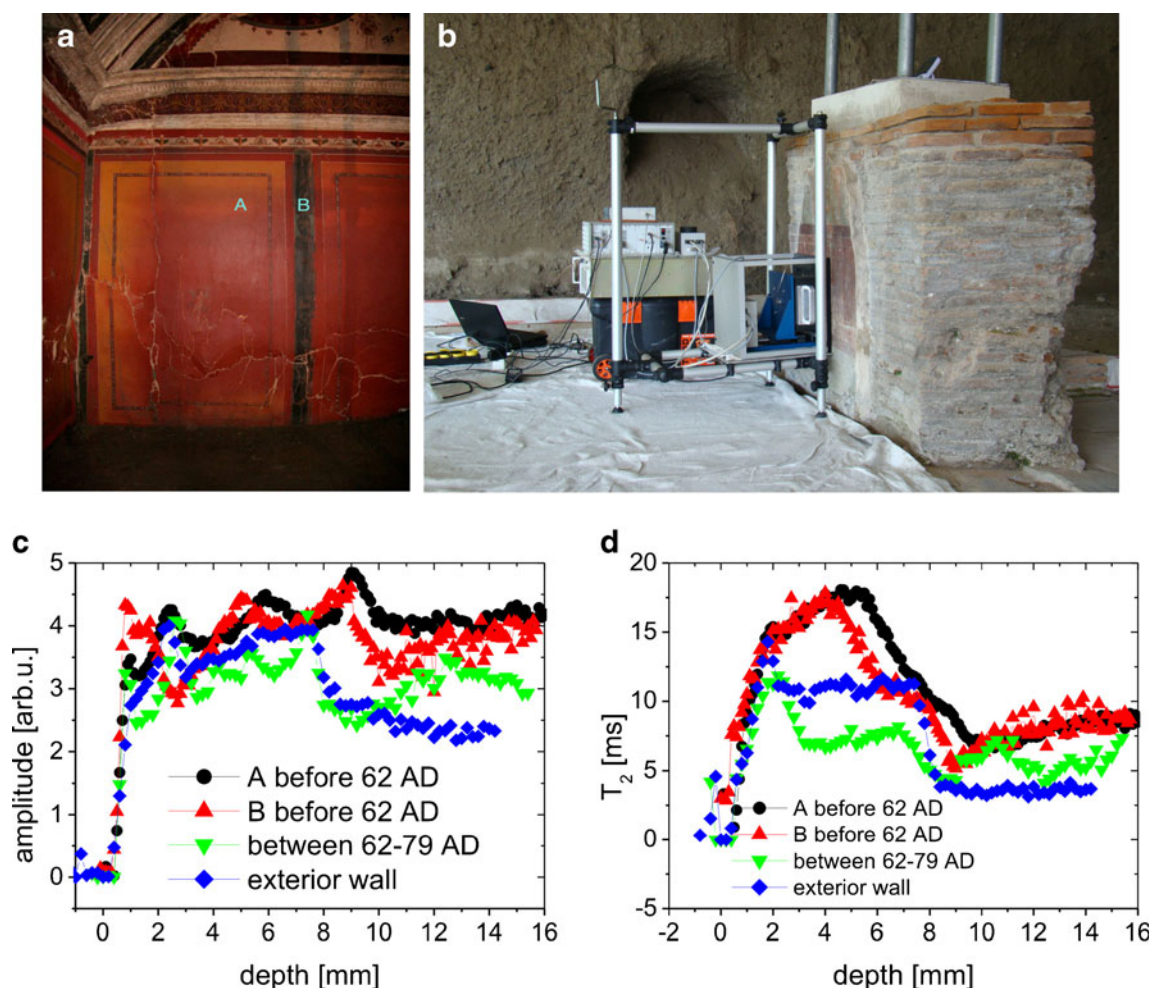
Fig. 4 NMR measurements at the Villa of the Papyri. **a**) Location of the measured points dating from before 62 AD. **b**) Experimental setup at the exterior wall on the terrace. **c**) Depth profiles at the four measured positions identifying different mortar layers and two different types of layer structures. **d**) T_2 profiles for all points measured. Different T_2 values are assigned to different mortar materials

was less expensive as much reconstruction work had to be executed after the earthquake, or the refined technique of crafting the more intricate mortar layers was in the process of or had already been lost. This interpretation suggests that also the outside wall of the terrace may have been reconstructed after the earthquake or that the technique used for outside walls had been applied for the reconstructed wall inside.

The NMR data clearly suggest that two different techniques were employed, which is in agreement with the XRF studies of the walls. Comparing the XRF spectra of the red pigments used for the restored and the original paintings shows that the restorers used cheaper red pigment as the spectrum of the restored wall shows a high iron content suggesting the use of iron oxide pigment to replace the highly expensive and precious intensely colored cinnabar (HgS), which is inferred by the presence of mercury and sulfur lines in the second spectrum. The

overlay of the XRF spectra of both walls is reported in Fig. 5a.

It is noted, that the two depth profiles recorded at the positions A and B differ in their moisture content in the first 3 mm. Profile A has been measured at a blank section of the painted wall, while profile B was taken on the painted vertical decoration. It is speculated that the decoration had been applied *a secco* so that the moisture uptake form the humid air is different in the two sections. This is also consistent as the FTIR spectra (Fig. 5b) of both surfaces are significantly different. Unfortunately the high moisture content made it difficult to investigate the presence of the C–H bending stretch at 3,000–2,800 cm^{-1} which would univocally determine the presence of an organic coating. However the presence of organic material on the vertical decoration (point B) can be indirectly inferred from the low intensity or lack of peaks at 2,500, 1,800, and 1,400 cm^{-1}, which would suggest the presence of a calcium carbonate

Fig. 5 Villa of the Papyri. **a**) XRF spectra. *Red*: Spectra of the red pigment on the wall built before 62 AD showing the presence of mercury (Hg) and sulfur (S) indicating that the red pigment used was cinnabar or mercury sulfide (HgS). *Blue*: Spectra or red pigment on the wall built after 62 AD, showing the absence of mercury and sulfur and the high content of iron (Fe) suggesting an iron red pigment such as hematite or red ochre. **b**) FTIR spectra. *Point B* reveals the possible presence of organic binder and oxalates, known to be degradation products of organic substances. *Point A* reveals stronger Calcium Carbonate bands suggesting that the technique is true fresco in this case
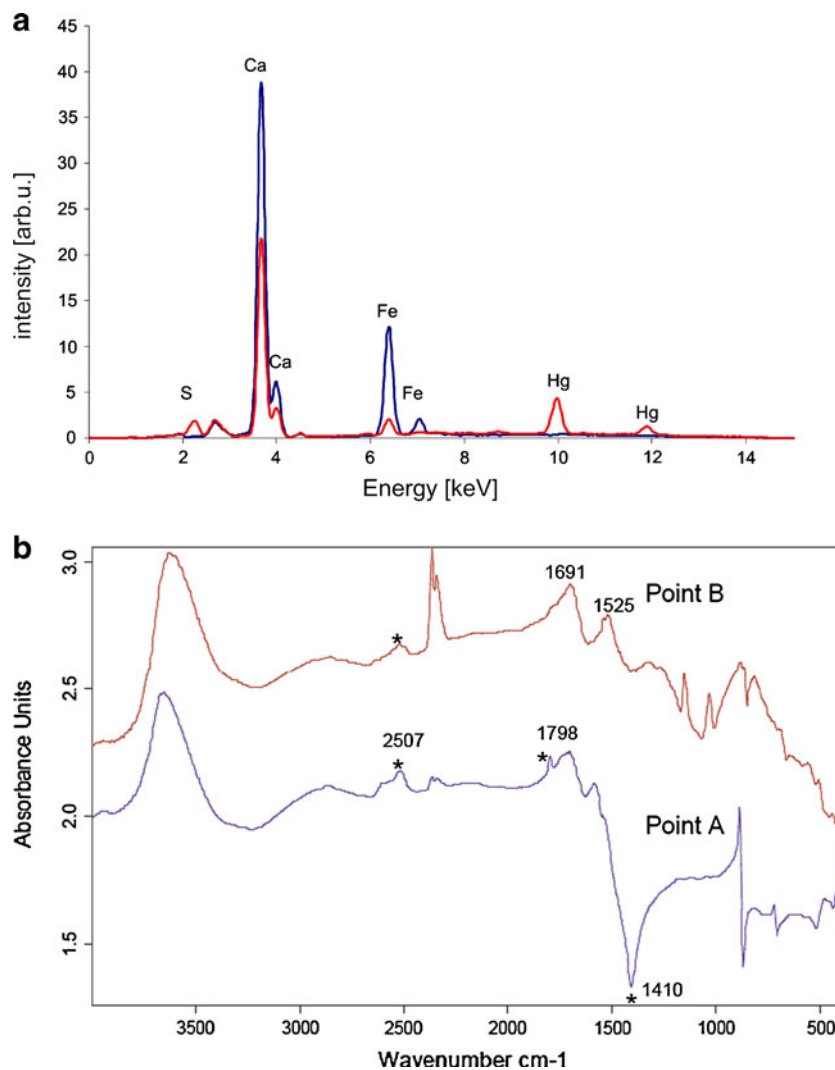
matrix, a strong indication that the technique used was true fresco. These bands are all present at point A, suggesting that the technique in point A was true fresco. Furthermore the spectrum of point B displays bands at about 1,691 and 1,525 cm^{-1}, which could indicate, in principle, the presence of a protein coating, although further studies need to be performed as the distortions observed in the region between 1,600 and 1,000 cm^{-1} complicate the interpretation of the spectrum.

Following Vitruvius [31], the mortar bed for wall paintings consists of three mortar layers, prepared with sand, followed by the application of three lime plaster layers prepared with marble dust. The painting is applied on the last layer, while still wet. Vitruvius recommends that the marble plaster layers be prepared with decreasing particle size towards the surface and to press them with a trowel to create a stronger surface by improving the packing density [31]. The packing of the layers coupled with the use of different aggregates (sand vs. marble dust) is likely to give rise to differences in the pore sizes across the mortar layer structure. Scientific analysis of

Roman wall paintings fragments has brought to light that other aggregates to prepare the mortar and plaster layers such as volcanic ash, ground brick, quartz, and clay were used depending on geography and budget, thereby showing variations of Vitruvius's recommendations [32]. Quartz and clay were found mixed with marble dust on the outermost layer in some of the wall fragments studied [32]. However, it is possible that in the case of the highly sophisticated and richly decorated Villa of the Papyri, Vitruvius' technique was closely followed in order to create the best paintings. We postulate that the last three layers give rise to the top three peaks observed up to a depth of 9 mm, beneath which the sand-mortar layers follow.

Similar to the amplitude profiles, the T_2 parameter profiles can also be grouped into the same two pairs (Fig. 4d). The T_2 profiles from points A and B differ only in the thickness of probably the second mortar layer which shifts the tail end of the profile of point B to the left when compared to the profile of point A. It is possible that the mortar with the second types of profiles was prepared with

Fig. 6 Distributions of relaxa-
tion times obtained by inverse
Laplace transformation of T_2
decays. a) T_2 distributions for all
measured points at 6 mm depth.
b) T_2 distributions at different
depths for the exterior wall
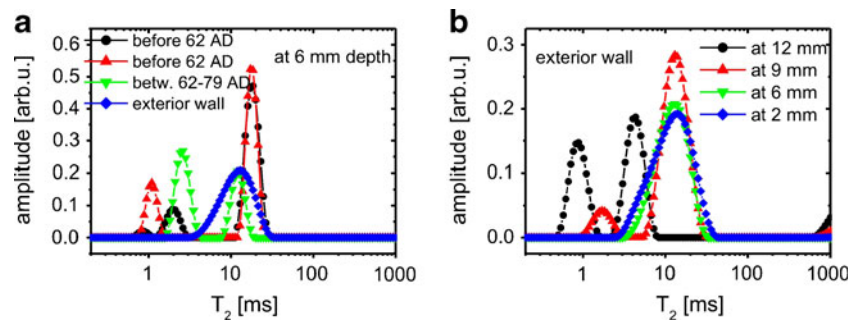
a different aggregate or mixture of aggregates. Based on the T_2 profiles, again at least two types of mortar layers can be identified. One type was used for the layers between 0 and 8 mm and another one for the layers further below. However, the layer between 6 and 8 or 9 mm (for the wall reconstructed between 62–79 AD) appears to give rise to an inconsistency to Vitruvius's rule because it gives rise to smaller T_2 values which could indicate smaller particle size or lower moisture content in the inner layers, especially in the case of the interior walls located in the newly excavated room which is kept at above 95% RH. Furthermore, a period of rain during the days before the measurements cannot be dismissed and could also account for the higher moisture content in the surface layers of the outer wall. The T_2 profile from the interior wall reconstructed between 62–79 AD shows high T_2 values in a thin surface layer, a lower T_2 plateau between 3 and 8 mm depth and even lower values further down. This general trend is followed by the profile from the terrace wall. But the initial peak is broader and the T_2 plateau is higher which is likely to be due to the different moisture content of the outside wall. Moreover, the structures appear at large depths which may arise from the different moisture balance.

Given the good signal-to-noise ratios of the data measured at the Villa of the Papyri, the measured CPMG decays could be inverted by inverse Laplace transformation to produce distributions of relaxation times T_2 (Fig. 6). This is a more refined analysis than fitting the measured signal with a model decay function such as a mono-exponential decay to extract a single relaxation time T_2 (cf. Fig. 4d). The T_2 distributions at a given depth of 6 mm at the four positions reveal again the similarities of the mortar structures identified in the depth

profiles above. Two peaks are observed, one at short relaxation times and one at long relaxation times. The one at short times can be assigned to bound water confined to small pores, while the one at long relaxation times is assigned to mobile water that partially fills larger pores. At 6 mm depth, this peak is basically identical for both positions A and B of the original wall and very similar for the restored wall and the outside wall (Fig. 6a). This similarity can be accounted for by the high moisture content of the atmosphere that the interior rooms are exposed to, and the period of rain to which the outer wall was exposed to in the days just before the measurements were taken. The peaks at short times seem to vary in an uncorrelated way, which may be due to the noise of the measurement data. The change of the T_2 distribution with depth reports the moisture content and pore structure in the different layers. The distributions spaced at 3 mm depth intervals for the outside wall indicate a systematic variation of the peak at large T_2 and a seemingly random variation for the peak at small T_2 (Fig. 6b). All peaks at large T_2 arise at the same position up to a depth of 9 mm indicating similarity of the mortar material across that range and a change towards larger depth.

The use of different types of mortar can also be seen by visual inspection of mortar pieces broken off the walls (Fig. 7a). A section from the Villa of the Papyri clearly shows a whitish first layer about 4 mm thick, followed by a somewhat darker layer up to 9 mm depth and slightly lighter colored mortar from thereon matching the profiles A and B from the older wall inside the Villa of the Papyri. As profiles ranging to up to 16 mm depth were not acquired from the much dryer walls of the Black Room, the initial parts of the profiles from the Villa of the Papyri

Fig. 7 a) Photo of a mortar
fragment from a fresco of the
Villa of the Papyri showing the
layer structure. b) Comparison
of depths profiles recorded from
walls in the Villa of the Papyri
and the Black Room for the first
6 mm
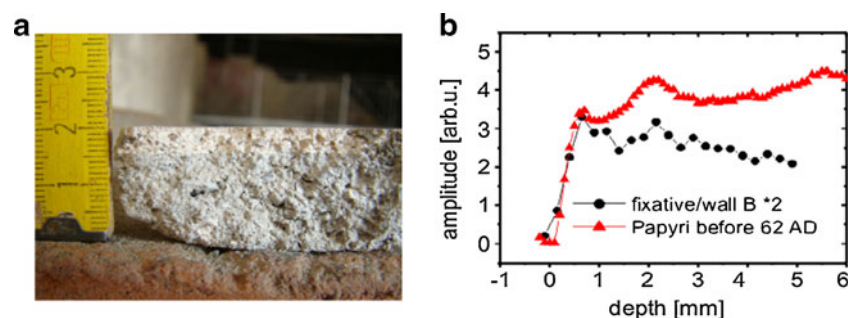
(point A) and the Black Room can be compared (Fig. 7b). The initial contours match, showing, that at least the outer mortar layers onto which the paintings were drawn are similar.

Conclusions

A noninvasive investigation of ancient wall paintings and mosaics was performed using the NMR-MOUSE®. For the measurements at the Mosaic of Neptune and Amphitrite differences between the tesserae and the mortar bed could be evidenced, and strong indications were found for an impregnation of the tesserae with an organic substance. The different conservation treatments and their influence on the moisture content in wall paintings in the Black Room were recorded, and the efficacy of each of the conservation treatments was estimated. The study shows that the conservation treatment with ammonium oxalate leads to lower moisture content of the wall, while the treatment with barium hydroxide leads to higher moisture content.

For the first time depth profiles of untreated, recently excavated wall paintings were taken in the Villa of the Papyri, which identified two different building techniques. The results of all of these measurements are expected on the one hand to help identify suitable conservation strategies and on the other hand to detect undocumented restoration efforts of the past. These studies demonstrate that NMR is a suitable tool to analyze and characterize the layer structures of different wall paintings and mosaics. By analyzing the proton content in terms of proton density and mobility, the NMR-MOUSE® provides a method for distinguishing layer structures and properties in a nondestructive way. Measurements taken in the same point but at different time periods demonstrate the accuracy and reproducibility of the measurements.

Moreover, in situ XRF studies coupled with reflectance FTIR spectra are in agreement with the NMR-MOUSE data and complemented the studies of the wall surfaces. It is shown that the NMR-MOUSE measurements coupled with in situ FTIR and XRF studies make a powerful nondestructive methodology to access the conservation treatments and the techniques of wall paintings.

References

1. Abragam A (1961) The Principles of Nuclear Magnetism. Clarendon Press, Oxford, UK
2. Blümich B (2005) Essential NMR. Springer, Berlin
3. Ernst RR, Bodenhausen G, Wokaun A (1987) Principles of Nuclear Magnetic Resonance in One and Two Dimensions. Clarendon Press, Oxford
4. Eidmann G, Savelsberg R, Blümler P, Blümich B (1996) J Magn Reson A 122:104–109
5. Perlo J, Casanova F, Blümich B (2005) J Magn Reson 176:67–70
6. www.act-aachen.de, accessed June, 2010
7. Bümich B, Casanova F, Perlo J, Presciutti F, Anselmi C, Doherty B (2010) Accounts Chem Res 43:761–770
8. Proietti N, Capitani D, Lamanna R, Presciutti F, Rossi E, Segre AL (2005) J Magn Reson 177:111–117
9. Proietti N, Capitani D, Rossi E, Cozzolino S, Segre AL (2007) J Magn Reson 186:311–318
10. Blümich B, Anferova S, Sharma S, Segre AL, Federici C (2003) J Magn Reson 161:204–209
11. Casieri C, Bubici S, Viola I, De Luca F (2004) Solid State Nucl Magn Reson 26:65–73
12. Proietti N, Capitani D, Pedemonte E, Blümich B, Segre AL (2004) J Magn Reson 170:113–120
13. Del Federico E, Centeno SA, Kehlet C, Currier P, Stockman D, Jerschow A (2010) Anal Bioanal Chem 396:213–220
14. Rühli FJ, Böni T, Perlo J, Casanova F, Baias M, Egarter E, Blümich B (2007) J Cult Herit 8:257–263
15. Proietti N, Capitani D, Cozzolino S, Valentini M, Pedemonte E, Princi E, Vicini S, Segre AL (2006) J Phys Chem B 110:23719–23728
16. Sharma S, Casanova F, Wachen W, Segre AL, Blümich B (2003) Magn Reson Imag 21:249–255
17. Blümich B, Casanova F, Perlo J, Anferova S, Anferov V, Kremer K, Goga N, Kupferschläger K, Adams M (2005) Magn Reson Imag 23:197–201
18. Blümich B, Casanova F, Perlo J (2008) Prog Nucl Magn Reson Spectrosc 52:197–269
19. Casieri C, Senni L, Romagnoli M, Santamaria U, De Luca F (2004) J Magn Reson 171:364–372
20. Blümich B, Haber A, Casanova F, Del Federico E, Boardman V, Wahl G, Stilliano A, Isolani I (2010) Anal Bioanaly Chem 397:3117–3125
21. Conservation and management of archaeological sites. Special edition on herculaneum (2007), 8.4
22. Matteini M (1992) in S. Cather (Editor) The Conservation of Wall Paintings, Getty Publications, 138–148
23. Matteini M (1999) The mineral approach to the conservation of mural paintings. Barium hydroxide and artificial oxalates, In: Conserving the painted past: developing approaches to wall painting conservation: post prints of an international conference organized by english heritage, 110–115
24. Carr HY, Purcell EM (1954) Phys Rev 94:630
25. Meiboom S, Gill D (1958) Rev Sci Instrum 29:688
26. Milliani C, Rosi F, Borgia I, Benedetti P, Brunetti BG, Sgamellotti A (2007) Appl Spectrosc 61:293–299
27. Rosi F, Daveri A, Miliani C, Verri G, Benedetti P, Pique F, Brunetti BG, Sgamellotti A (2009) Anal Biolanal Chem 395:2097–2106
28. Miliani C, Rosi F, Burnstock A, Brunetti BG, Sgamellotti A (2007) Appl Phys A 89:849–856
29. Garcia Manzano C (2010) Characterization by XRF of the Neptune and Amphitrite Roman Mosaic at Herculaneum, Italy. Unpublished MS tesis, Hunter College, Pratt Institute
30. Gallagher W (2007) FTIR analysis of protein structure http://www.chem.uwec.edu/Chem455_S05/Pages/Manuals/FTIR_of_proteins.pdf, accessed January 2011

31. Vitruvius MP (1999) Ten Books on Architecture [De architectura libri decem]. Cambridge University Press

32. Donner O (1869) Die erhaltenen antiken Wandmalereien in technischer Beziehung. Breitkopf und Härtel, Leipzig

33. Del Federico E, Blümich B, Haber A, Garcia Manzano C, Boardman V, Souvorova D. "Non-Destructive Multianalytical characterization of Roman Polychorme Mosaics". Manuscript in preparation

34. Roman Wall Paintings: Materials, Techniques, Analysis and Conservation. Proceedings of the International Workshop on Fribourg 7–9 March 1996. Editors, H. Béarat, M. Fuchs, M. Maggetti, D. Paunier